ISTITUTO NAZIONALE DI FISICA NUCLEARE - ISTITUTO NAZIONALE DI FISICA NUCLEARE - ISTITUTO NAZIONALE DI FISICA NUCLEARE - ISTITUTO NAZIONALE DI FISICA NUCLEARE - ISTITUTO NAZIONALE DI FISICA NUCLEARE - ISTITUTO NAZIONALE DI

Laboratori Nazionali di Frascati

Submitted to Nucl. Inst. & Meth. in Phys. Res.

LNF-94/015 (P)
16 Marzo 1994

V. Patera, M. Carboni, G. Battistoni, A. Ferrari:

SIMULATION OF THE ELECTRO-MAGNETIC COMPONENT OF EXTENSIVE AIR SHOWERS

PACS.: 96.40.Pq

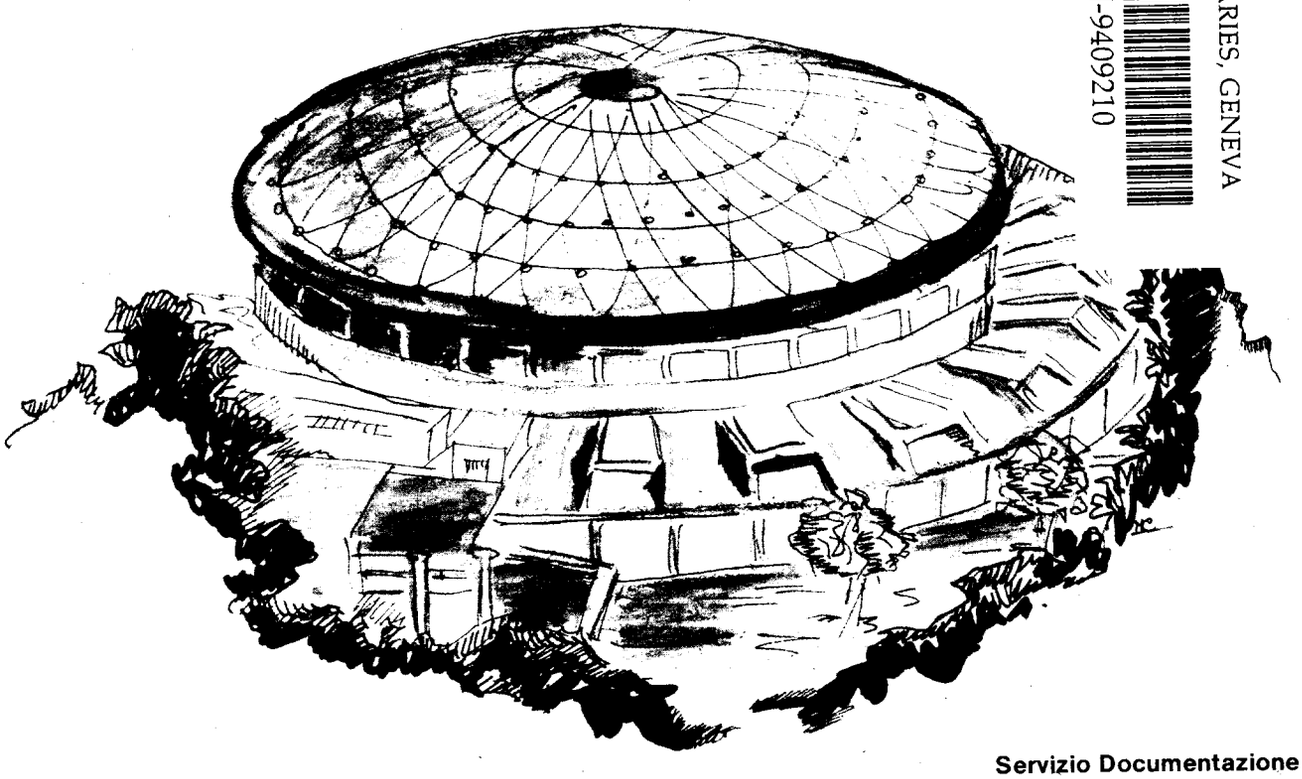

Servizio Documentazione
dei Laboratori Nazionali di Frascati
P.O. Box, 13 - 00044 Frascati (Italy)

INFN - Laboratori Nazionali di Frascati
Servizio Documentazione

LNF-94/015 (P)
16 Marzo 1994

SIMULATION OF THE ELECTRO-MAGNETIC COMPONENT OF EXTENSIVE AIR SHOWERS

V.Patera[+], M.Carboni
INFN - Laboratori Nazionali di Frascati, P.O.Box 13, I-00044 Frascati
[+] Dipartimento di Energetica, Facolta' di Ingegneria dell' Universita' di Roma "La Sapienza".

G.Battistoni, A.Ferrari
INFN - Milano, via Celoria 16, I-20133 Milano

Abstract

The e.m. component of Extensive Air Showers, as sampled at a given atmospheric depth, may be considered as the superposition of sub-showers initiated by photons and electrons(positrons) mainly coming from the decay of secondary mesons. A detailed simulation of showers in atmosphere as produced by gammas and electrons has been performed by means of standard high energy physics Monte Carlo codes. We developed a set of parametrisations of these sub-showers to be included in the full simulations of Extensive Air Showers with the aim to reduce the required computer power. Comparison with previous results found in the literature are shown.

1 Introduction

The experiments measuring Extensive Air Showers (EAS) nowadays have reached a high level of complexity and sizeable dimensions, producing a corresponding increase in the quality and statistics of the experimental data. The analysis of such high quality data needs adequate simulations of the shower development in the atmosphere and of the response of the detector.

The accurate simulation of a large number of EAS produced by primary nuclei with energy ranging up to 10^5 TeV and beyond [1] is a formidable task in terms of computing power. On the other hand most of the present cosmic ray shower generators [2] provide the opportunity to follow the secondary particles produced at different depths in the atmosphere (e.g. photons from π^0 decay, electrons from semileptonic decays of K, etc.). In order to maintain computer time within reasonable limits, these secondaries are followed down to a suitable, not too low, energy threshold. It is then assumed that each of these secondaries originates a sub-shower contributing to the total e.m. "size" measured by air shower arrays. The average number of electrons/positrons arriving at the depth of the shower array from each sub-shower is often derived from existing analytical shower approximations [3]. Fluctuations of individual sub-showers are usually neglected, due to the common belief that they are overwhelmed by the fluctuations in the development of the Extensive Air Shower itself.

This work originates from the need to test the range of validity of these analytical approximations. Furthermore, a known limit of the quoted formulae is that they are constructed to give a number of equivalent charged particles, but real experiments, like those based on arrays of scintillators, are also sensitive to the conversion of gamma rays, which are known to dominate the shower development beyond the maximum. In a practical situation, if thick scintillator counters are used, a significant number of these photons will interact in the sensitive medium, contributing to the detected signal. This effect is also known as "Transition effect", after the work of Rossi and Greisen [4]. In the analysis of experimental data an estimated correction factor is usually inserted. Therefore it is useful to give expressions for the number of secondary electrons/positrons and gammas separately, together with their energy distributions. A detailed simulation of the number of electrons and positrons in air showers from different primaries can already be found in [5].

In this work we have used specialised shower programs commonly used in high energy physics to extract a set of parametrisations to describe the sub-showers initiated by secondary particles at different energies and different depths in the atmosphere. We obtained the number of secondary particles, its fluctuations, and the energy distribution of secondaries, for gamma-initiated sub-showers in the energy range $10 \div 10^5$ GeV, and for electrons-initiated sub-showers in the energy range $10 \div 10^4$ GeV, as a function of atmospheric depth ranging up to about 27 X_0. The motivation to limit the energy range of electron-initiated sub-showers with respect to the case of gamma-initiated ones stems from an analysis of the energy distribution of secondary particles in EAS according to the HEMAS simulation code[6]. The above mentioned features of the electro-magnetic cascade allow to express the results in terms of the total thickness expressed in radiation length, independently from $X_{detector}$ and X_{start}.

We remark the importance of taking into account fluctuations. As already reported by other authors [7], biases are introduced in the final results when using only the average values. This is due to the non-symmetric shape of distributions of the number of secondary particles.

In the next section we describe the simulation tools. The results are then reported in section 3.

2 The simulation

Among the shower programs available in the High Energy Physics community, we have adopted GEANT version 3.15 [8] and FLUKA [9]. For primary energy greater than a few TeV FLUKA has been mainly used, since there GEANT starts to exit from its range of validity. We have verified that at the boundary energies around 10^3 GeV the results of the two generators in air are reasonably compatible, as discussed later.

The simulations have been performed on different platforms (HP-UX, IBM-AIX, VAX, and ALPHA DECStations).

The atmosphere is defined by a stack of box volumes of rectangular basis and thickness increasing with the height above the sea level. Any volume corresponds to a depth of $\sim 24\ gr/cm^2$. In each box the density is uniform, and it is chosen in such a way that an approximation to the standard U.S. atmosphere is performed according to the Shibata fit[10]. The chosen depth granularity in our approximation is about one half of radiation length ($37.66\ gr/cm^2$) in air. The exact relation between height and slant depth is shown in Fig. 1, with the polygonal representing our approximation.

We have limited the top of atmosphere at $5\ gr/cm^2$ (corresponding to a vertical height of $\simeq$ 36 Km), and the bottom is at $1025\ gr/cm^2$ (corresponding to the sea level). We have used the same elemental composition at all depths.

We have fixed the kinetic energy cut for secondary particles to 1 MeV. This is an improvement with respect to the results of ref. [5], where the lowest considered cut, for electrons, was 5 MeV. It turns out that, in practice, a 1 MeV threshold is a reasonable compromise, taking into account both the quality of the results and the required computer time. In fact, one has to consider that real detectors are often shielded by an amount of material capable of absorbing most of low energy (less than 1 MeV) secondary electrons. The matter could be different, in principle, for low energy secondary photons which have a longer transmission coefficient, but the electrons are those which are responsible for most of the energy deposition in an active material.

At very high energy we made use of the possibility offered by FLUKA to exploit biasing techniques in order to explore with good accuracy the longitudinal profile in a reasonable time, although this did not allow to measure the correct fluctuations, which were studied with analogical simulations at lower statistics.

We also did not change the energy threshold in the different air layers, otherwise it would have not be possible to parametrise the results as a function of the atmospheric thickness expressed in radiation lengths, independently from $X_{detector}$ and X_{start}, taken separately.

An example of the simulation set-up is given in Fig. 2 which shows the development of a shower initiated by an electron of 300 GeV starting at a vertical atmospheric depth of $60\ gr/cm^2$; only secondary tracks with energy greater than 500 MeV are shown for clarity. In order to achieve a reliable parametrisation of the relevant shower properties, we generated sub-shower at different log-spaced energies: 10, 18, 31, 56, 100, 177, 316, 562, 1000, 1778, 3128, 5623, 10000, 17780, 31620, 56230, 100000 GeV (the last four values have been omitted for electron showers), and at 16 different starting depths: from 10 to 910 gr/cm^2, in 60 gr/cm^2 steps.

3 Results

We have considered as interesting quantities the longitudinal profile together with the associated fluctuations, the energy distribution of secondary particles above the Monte Carlo cut, and their lateral distribution. In this paper we shall not explore the details of the lateral distribution, limiting ourselves to some general considerations. This topic will be treated separately in a forthcoming dedicated paper together with the analysis of arrival times and of their fluctuations as a function of radial distance from the shower axis.

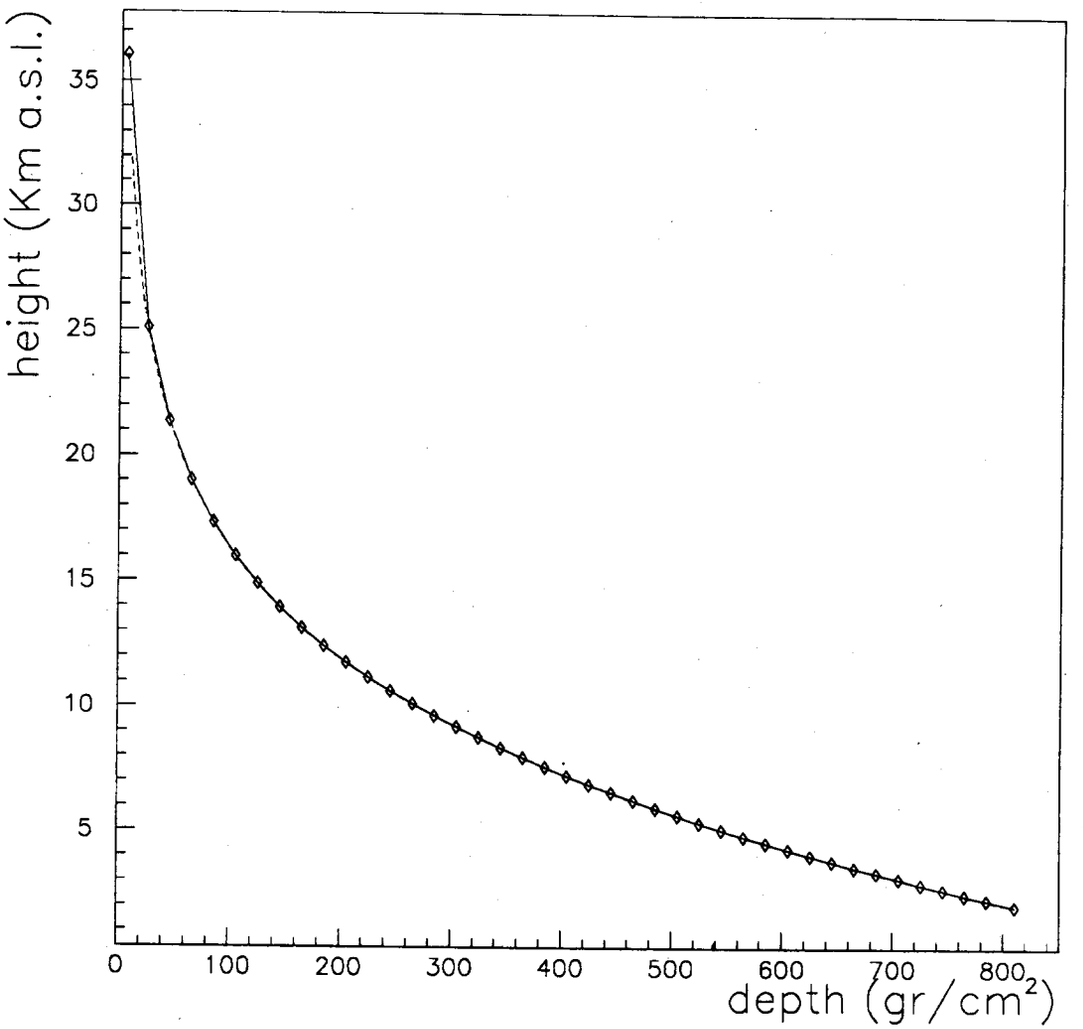

Figure 1: *The profile of the standard atmosphere used in the simulation set-up. The solid line is the adopted piece-wise linear approximation.*

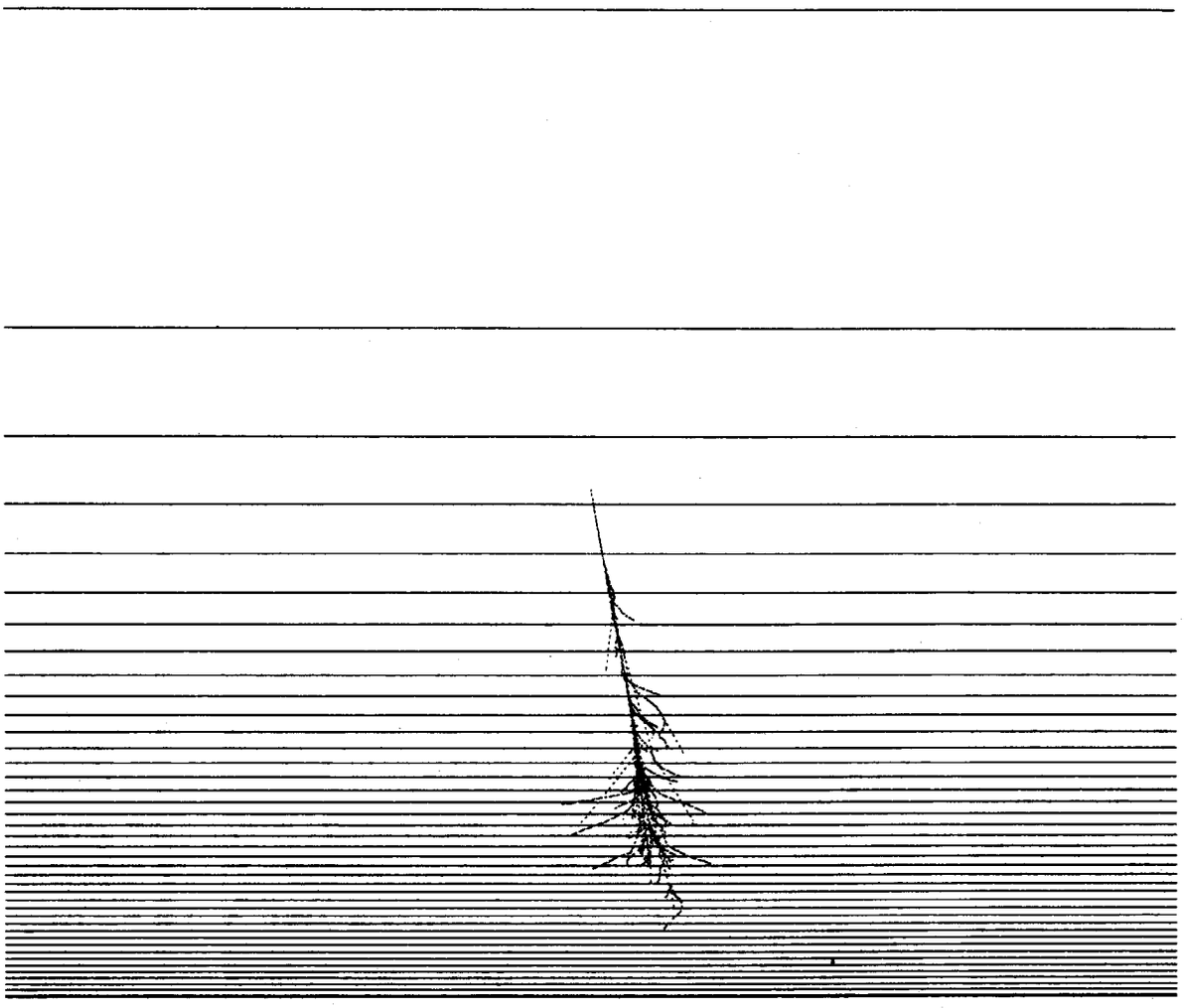

Figure 2: *A 300 GeV electron shower in atmosphere, initiated at 60 gr/cm^2, as simulated using GEANT. (only secondaries with energy greater than 500 MeV are shown). The box structure reproducing the atmosphere, from 2 km to 36 km above sea level, is shown: each layer has a thickness of about 0.5 X_0. The horizontal scale is enlarged by a factor of 100 with respect to the vertical*

We have fitted the Monte Carlo results with phenomenological parametrisations, trying to minimise as much as possible the number of parameters. Whenever possible we started from the analytical expressions already existing in the literature, so that the possible differences with respect to the simplified shower theory could emerge naturally.

3.1 Longitudinal profiles

We sample the longitudinal profile by counting the number of secondary particles crossing the boundary between the adjacent air regions in our simulation set-up. We have fitted the number of secondary e^+e^- or photons, with energy greater or equal to the Monte Carlo cut (1 MeV) using a six parametres expression similar to that proposed by Greisen[11]:

$$< N_{e,\gamma}(E_0,t) >= C_1 \cdot \beta^{C_2} \cdot e^{t_1 \cdot (C_5 - C_6 \cdot \log s_1)} \tag{1}$$

where

$$t_1 = t - C_4 \tag{2}$$

$$\beta = \log\left(\frac{E_{primary}}{\epsilon_C}\right) \tag{3}$$

$$s_1 = \frac{3 \cdot t_1}{t_1 + C_3 \cdot \beta} \tag{4}$$

t being the atmospheric depth expressed in radiation lengths, and ϵ_C the critical energy in atmosphere: $\sim 81 MeV$. The variable s_1 is therefore a slightly modified "age" parameter. The exact definition of the age parameter can be found in the quoted ref. [11], we just remind here that it is an dimensionless number emerging in the analytical treatment of atmospheric showers. It ranges approximately between 0.5 and 2.0, according to the distance from the first interaction, reaching the unit value at the shower maximum.

We want to remark THAT this single formula is able to provide a good approximation of the longitudinal profiles in the whole considered energy range (5 orders of magnitude).

All C_i $(I = 1, 2, ..., 6)$ parameters depend upon both primary and secondary nature. They are given in Tables 1 and 2.

Secondary	C_1	C_2	C_3	C_4	C_5	C_6
e^+e^-	.21915	-.38502	1.7709	-.041189	1.1189	1.5532
γ	.85721	-.15412	1.9988	-.43781	.97262	1.4218

Table 1: *Parameters of the fit to the longitudinal shower profiles for gamma-initiated sub-showers*

Secondary	C_1	C_2	C_3	C_4	C_5	C_6
e^+e^-	.33499	-.73003	1.4908	.3046	1.3639	1.7703
γ	1.169	-.34014	1.7893	-.076683	1.0986	1.5324

Table 2: *Parameters of the fit to the longitudinal shower profiles for electron-initiated sub-showers*

An example of the quality of the fits to the longitudinal profiles for a few primary energies is given in Fig. 3 and 4 for photon- and electron-initiated sub-showers respectively. Some

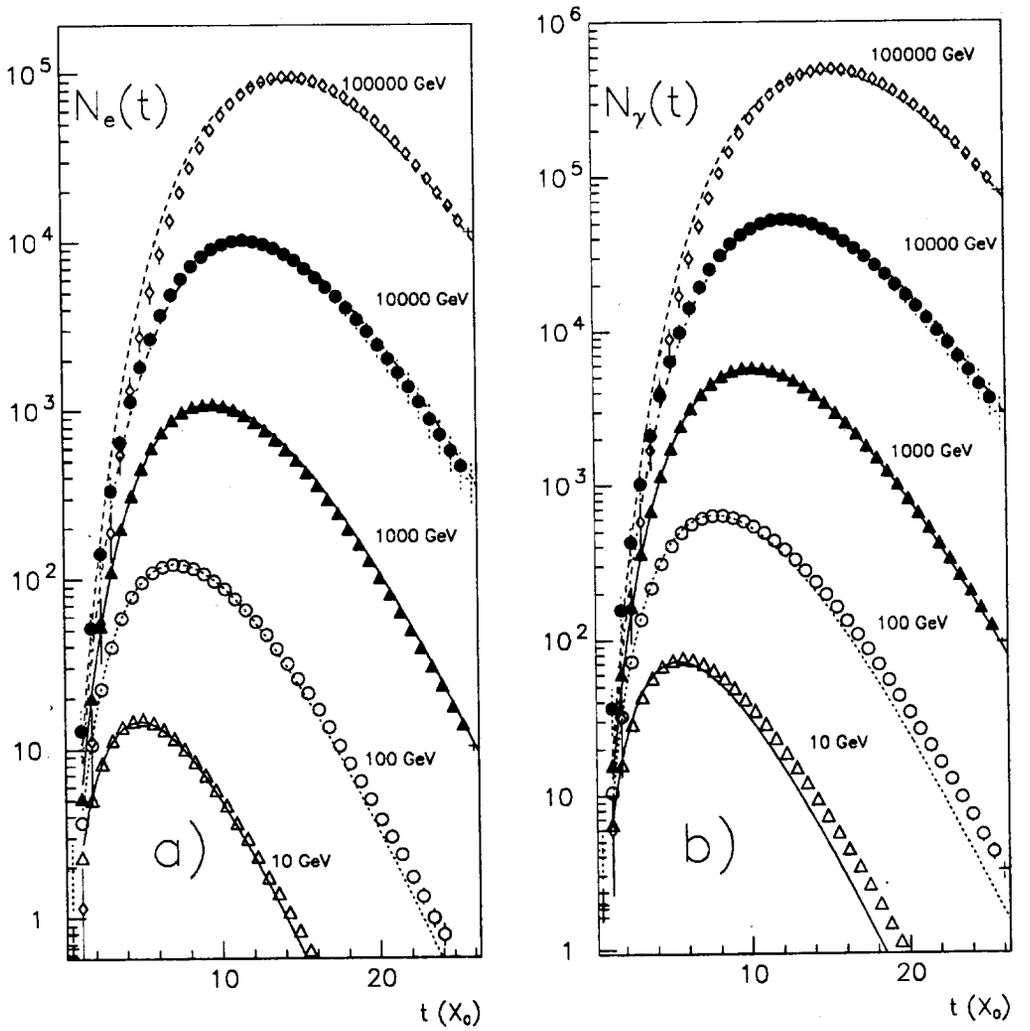

Figure 3: *a) Longitudinal profiles of secondary electron/positrons from gamma-initiated subshowers, 0.01, 0.1, 1, 10, and 100 TeV primary energy; b) longitudinal profiles of secondary photons. The results of expression 1 are superimposed.*

systematic tendency to underestimate the real profile may appear beyond the shower maximum, in particular for γ secondaries at the lower primary energies. However, we have verified that such deviations are within the fluctuations of the performed simulation.

It is interesting to notice how C_5 is always not far from 1, and C_6 is about 3/2, as expected in Greisen theory. Instead the meaning of parameter C_4 is linked to the known differences in shower development for electrons and photons.

From expression 1 we also derive the position of shower maximum as a function of energy:

$$t_{max} = \frac{(1 + x_m) \cdot C_3 \cdot \beta}{2 - x_m} - C_4 \tag{5}$$

where

$$x_m = \frac{2}{3}\left(1 - \sqrt{4 - \frac{9}{2}\frac{C_5}{C_6}}\right) \tag{6}$$

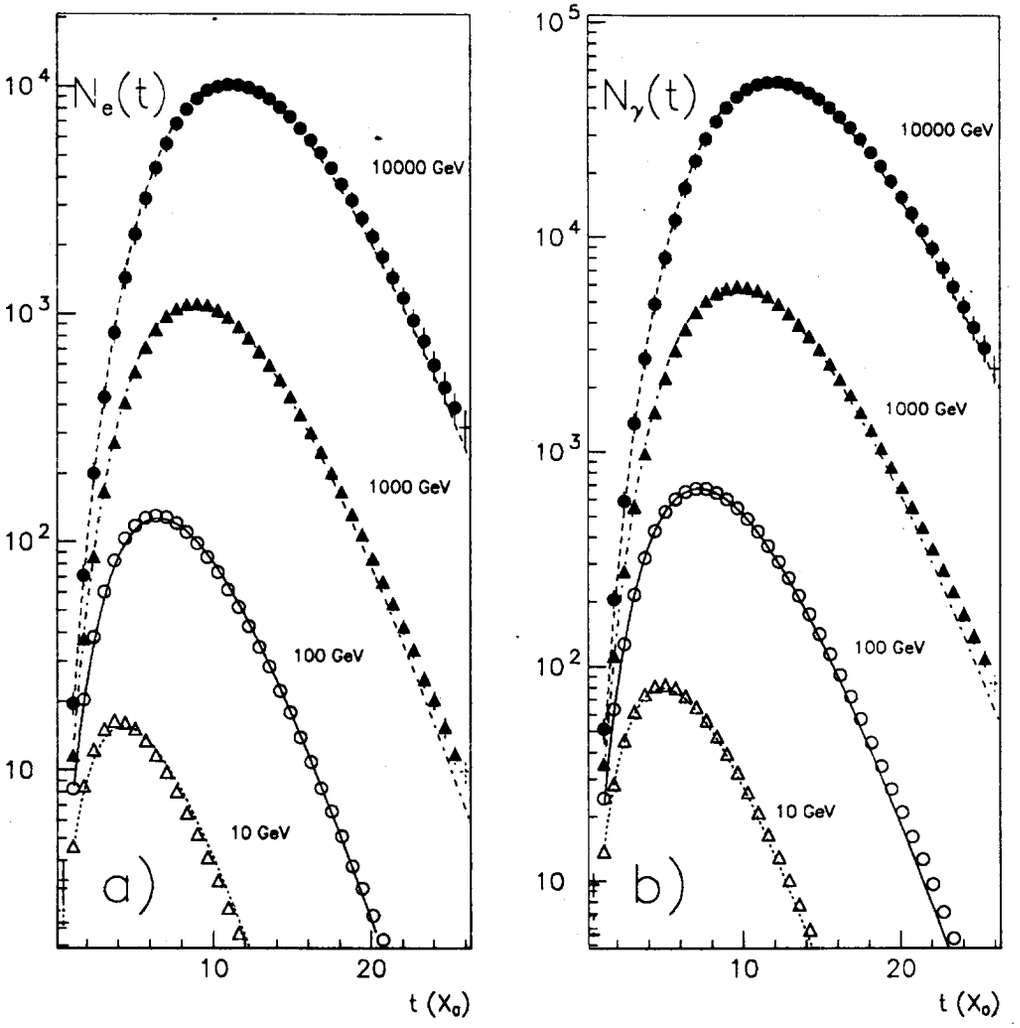

Figure 4: *a) Longitudinal profiles of secondary electron/positrons from electron-initiated sub-showers, 0.01, 0.1, 1, and 10 TeV primary energy; b) longitudinal profiles of secondary photons. The results of expression 1 are superimposed.*

The above formulae are obtained knowing that around the maximum $s_1 = 1 + x_m$, with $x_m << 1$, and then using the Taylor expansion of $\log(1+x)$ up to second order. As expected t_{max} grows linearly with β, i.e. with $\log E_0$.

In Fig. 5 we show the depth at which the shower maximum is reached in the Monte Carlo results, as a function of $\log_{10} E_0$, for gamma-initiated sub-showers. In the region 1-10 TeV the results of GEANT and FLUKA are superimposed. It can be noticed how the GEANT results start to deviate from the expected linear behaviour after a few TeV. At lower energy both codes give, with remarkable approximation, the same results, as shown in Fig. 6 for 1 TeV gamma-initiated sub-showers.

We also compare our results to other parametrisations existing in the literature. In fig. 7 our Monte Carlo results for 1 TeV gamma- and electron-initiated sub-showers, for an energy cut of 5 MeV, are compared to the parametrisation of ref. [5], where the same cut was used.

It is clear how the formula given in ref. [5] gives a reasonable account of the charged particles, but it is self-evident the importance of secondary photons. The fraction of energy deposition in the sensitive material due to these photons will depend of course on the atomic characteristics of the medium and on its thickness.

3.2 Fluctuations

In order to parametrise the fluctuations on the number of secondary particles, we have tried, at phenomenological level, to take into account the fluctuations on the starting point of the showers. This brings naturally to search for a function of the age parameter as suggested in ref. [3]. However, a Poisson-like term seems unavoidable, in particular beyond the shower maximum. Valuable results have been obtained by us using the following expression:

$$\frac{\sigma^2_{N_{e,\gamma}(E_0,t)}}{< N_{e,\gamma}(E_0,t) >^2} = k_1^2 \cdot [s_1 - k_2 - k_3 \cdot \log(s_1)]^2 + \frac{k_4}{< N_{e,\gamma}(E_0,t) >} \tag{7}$$

where $< N_{e,\gamma}(t) >$ and s_1 are respectively the average number of secondaries and the modified age parameter as defined in section 3.1. The k_i factors are functions of primary energy, and depend also on the nature of primary and secondary particles. Examples of the results are summarised in Fig. 8 and 9 for gamma- and electron-initiated sub-showers respectively.

In order to make use of these parametrisations, one has to consider that the number of secondary particles is log-normally distributed, with good approximation. It can be easily shown that the following relations hold[12]:

$$\sigma^2_{\log N} = \log\left[\frac{\sigma^2_N}{< N >^2} + 1\right] \tag{8}$$

$$< \log N >= \log < N > - \frac{\sigma^2_{\log N}}{2} \tag{9}$$

The k_i parameters with $i = 1, 2, 3$ can be defined as polynomials of the variable $y = \log_{10}(E_0)$

$$k_i = W_0^i + W_1^i \cdot y + W_2^i \cdot y^2 \qquad i = 1, 2, 3 \tag{10}$$

while for the 4-th parameter k_4 we have :

$$k_4 = \exp\left(W_0^4 + W_1^4 \cdot y + W_2^4 \cdot y^2\right) \tag{11}$$

The W_i^j parameters are given in Tab. 3 and 4 for γ and e^+e^- primaries and secondaries.

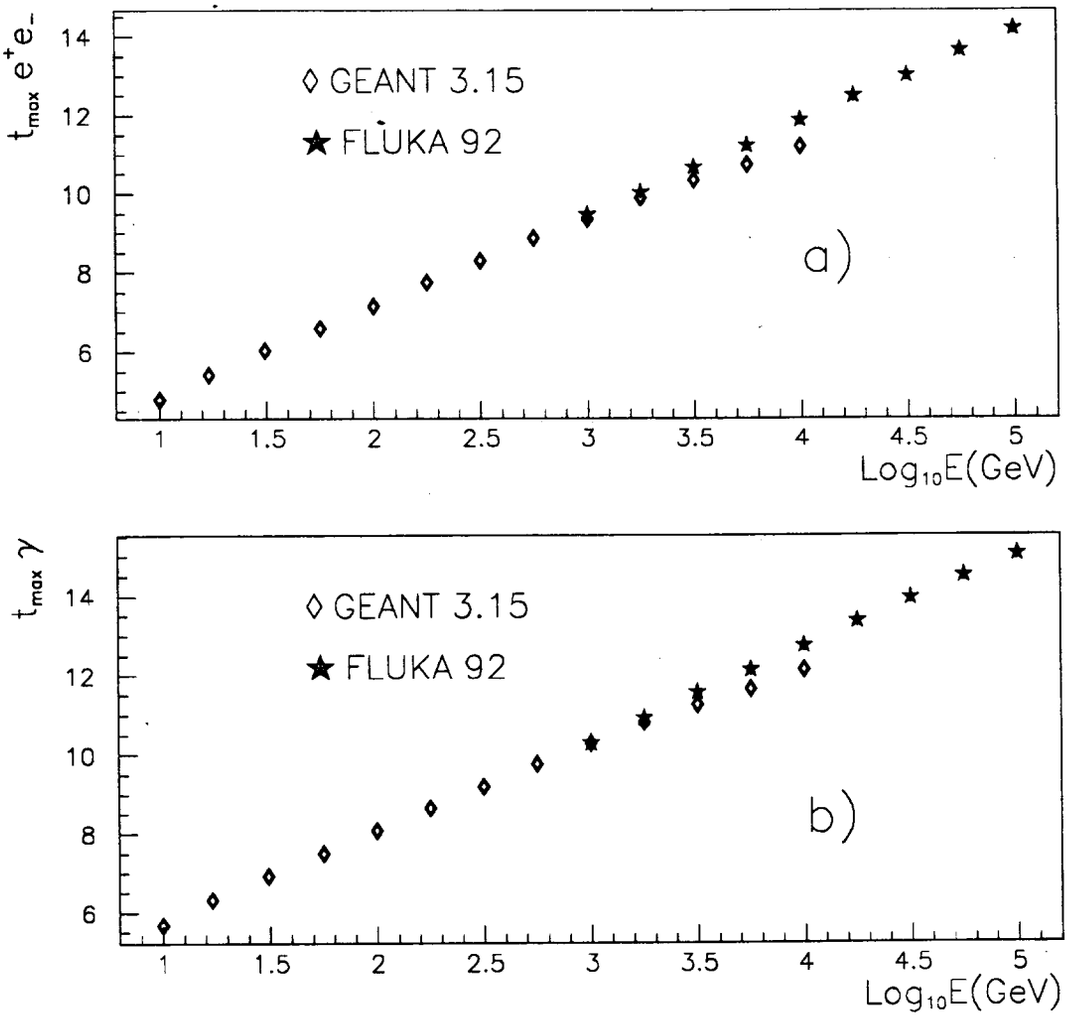

Figure 5: *Atmospheric depth at which the shower maximum is reached, as a function of* $\log_{10} E_0$*, for gamma-initiated sub-showers; a) secondary* e^+e^-*, b) secondary* γ*. In the energy region* $10^3 - 10^4$ *GeV GEANT and FLUKA results are superimposed: FLUKA is able to maintain the linear behaviour even at these high energies.*

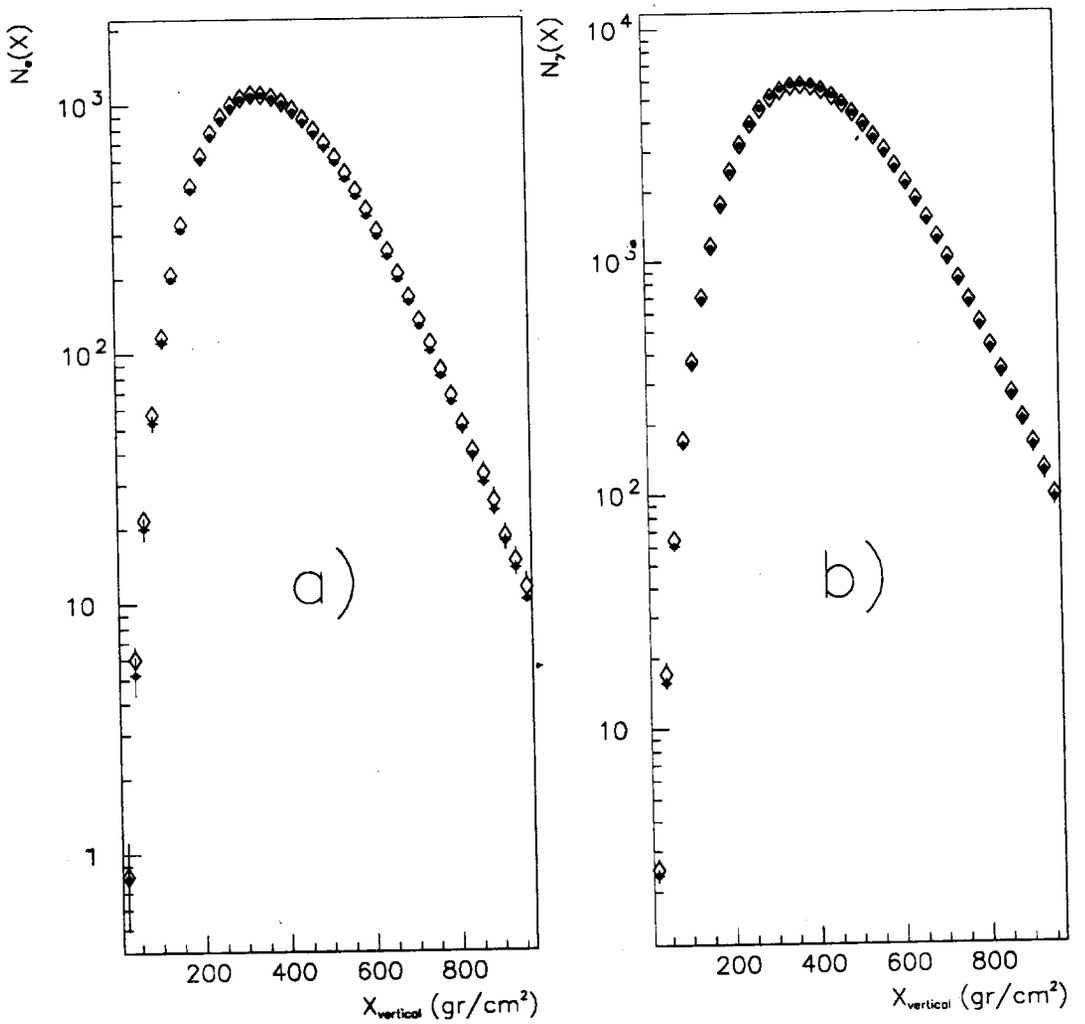

Figure 6: *Longitudinal profiles of secondary electrons (a), and of secondary photons (b), for simulated 1 TeV gamma-initiated sub-showers, as a function of atmospheric depth. Black symbols are the GEANT results, while the open ones are from FLUKA*

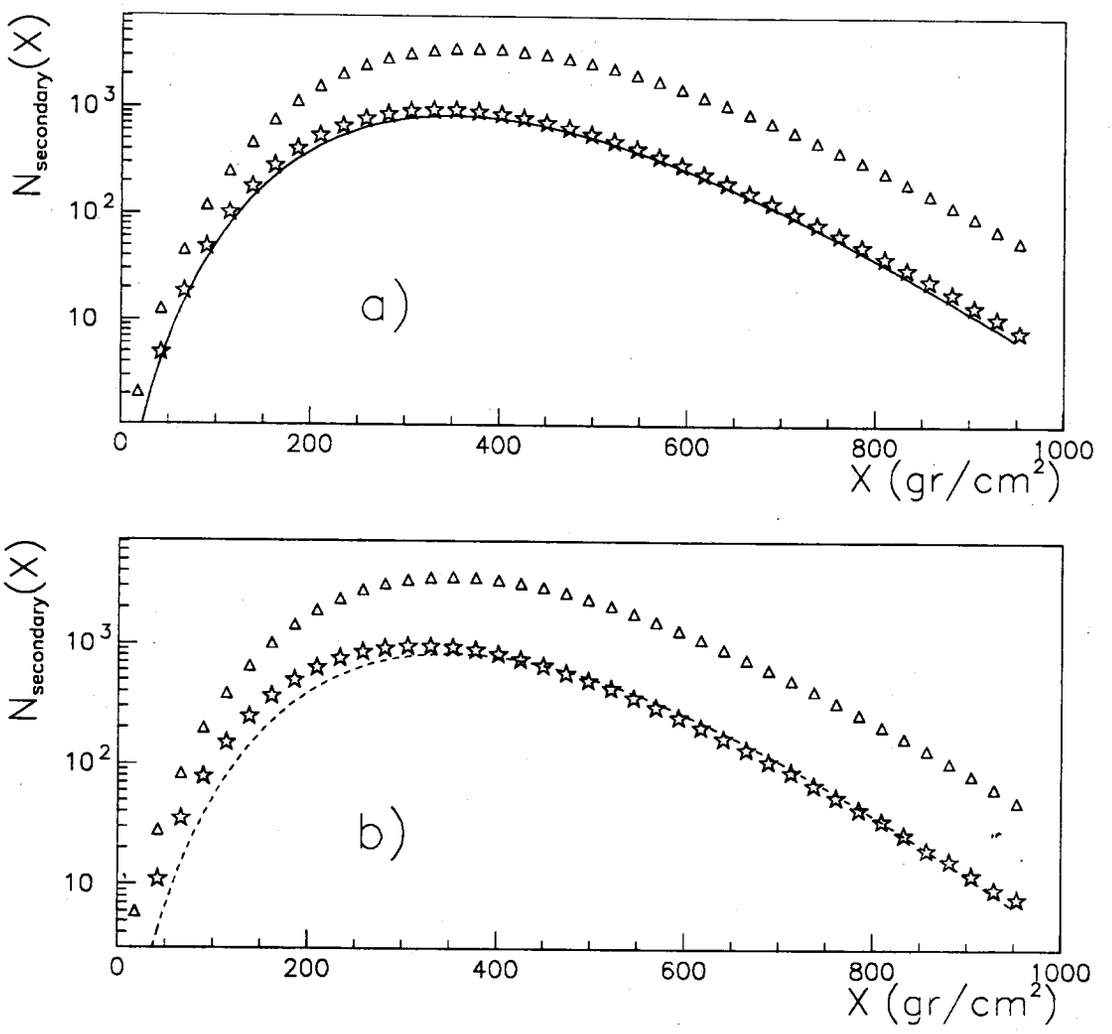

Figure 7: *Longitudinal profiles of secondary electron (stars) and gammas (triangles) of energy $\geq 5MeV$ for 1 TeV gamma showers (a), and electron showers (b), initiated at 10 gr/cm^2. The continuous and dotted lines are the analytical prediction for secondary electrons given by E.J. Fenyves et al.*

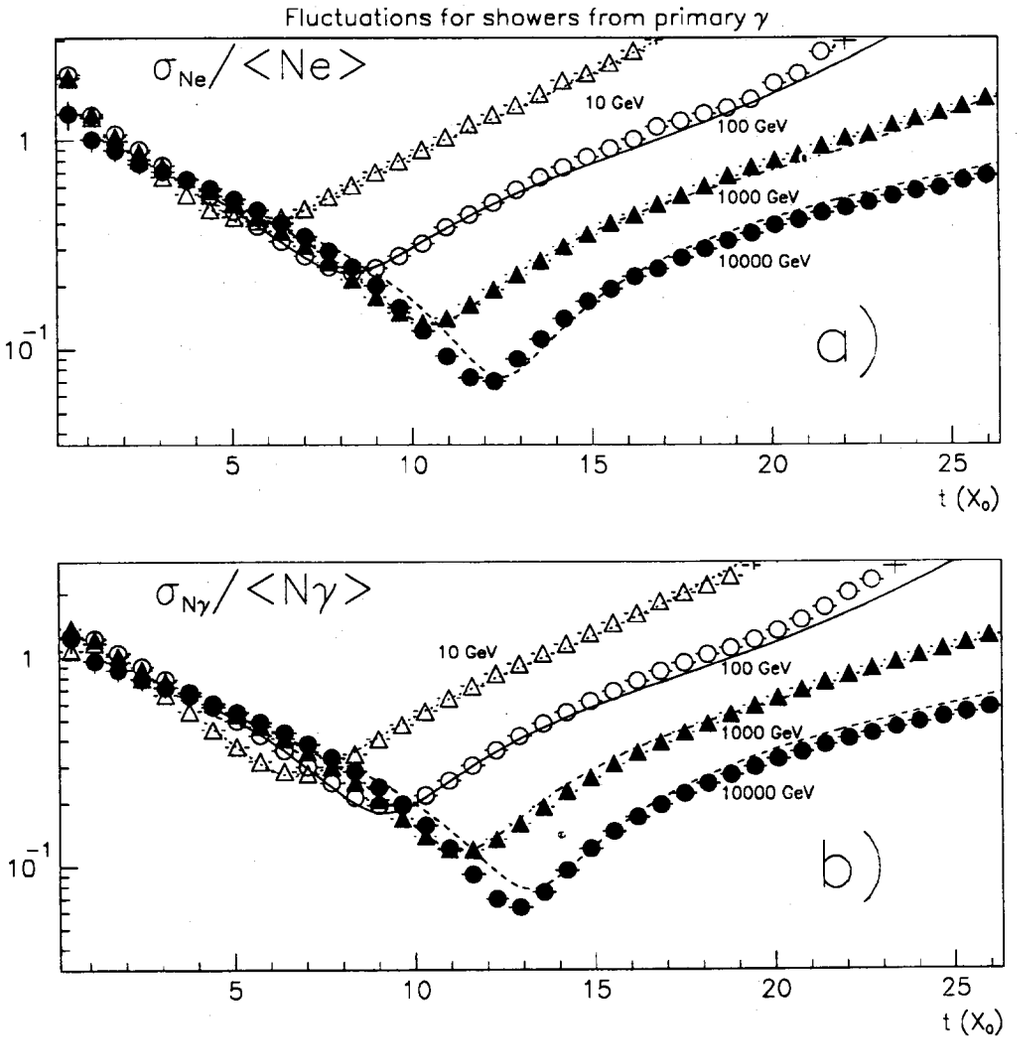

Figure 8: ***Relative fluctuations of of secondary e^+e^- (a) and γ (b) ($E \geq 1$ MeV) for gamma initiated sub-showers as a function of atmospheric depth in r.l.***

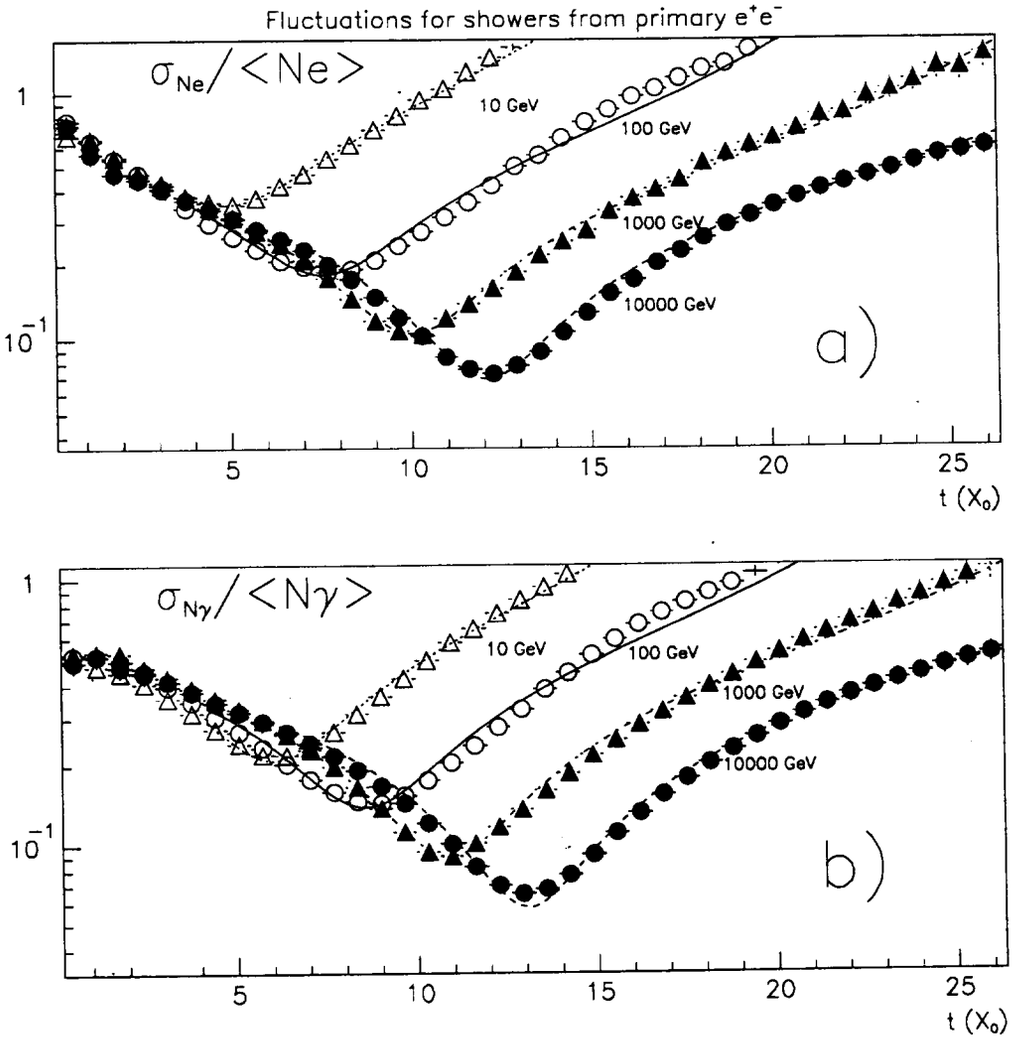

Figure 9: *Relative fluctuations of of secondary e^+e^- (a) and γ (b) ($E \geq 1$ MeV) for electron initiated sub-showers as a function of atmospheric depth in r.l.*

γ initiated						
	e^+e^- secondary			photons secondary		
Coeff.	W_0	W_1	W_2	W_0	W_1	W_2
k_1	1.81	0	0	1.31	$3.38 \cdot 10^{-1}$	$-6.22 \cdot 10^{-2}$
k_2	1.19	$-3.00 \cdot 10^{-2}$	0	1.21	$-6.38 \cdot 10^{-1}$	$4.92 \cdot 10^{-3}$
k_3	$2.94 \cdot 10^{-1}$	$4.30 \cdot 10^{-2}$	0	$2.80 \cdot 10^{-1}$	$3.30 \cdot 10^{-2}$	0
k_4	$-2.99 \cdot 10^{-1}$	1.07	0	$1.81 \cdot 10^{-1}$	1.39	0

Table 3: *Fit parameters for the fluctuations of the longitudinal profile for γ-initiated sub-showers*

e^+e^- initiated						
	e^+e^- secondary			photons secondary		
Coeff.	W_0	W_1	$W_2 \times 10^3$	W_0	W_1	$W_2 \times 10^3$
k_1	2.97	$-5.58 \cdot 10^{-1}$	49.4	1.72	$1.13 \cdot 10^{-1}$	-46.2
k_2	1.04	$4.25 \cdot 10^{-2}$	-6.77	1.13	$-2.20 \cdot 10^{-2}$	2.28
k_3	$9.30 \cdot 10^{-1}$	$-1.11 \cdot 10^{-1}$	9.75	$6.67 \cdot 10^{-1}$	$2.49 \cdot 10^{-3}$	-8.19
k_4	$1.96 \cdot 10^{-1}$	$2.73 \cdot 10^{-1}$	161	$-1.74 \cdot 10^{-1}$	1.34	-1.34

Table 4: *Fit parameters for the fluctuations of the longitudinal profile for e^+e^--initiated sub-showers*

3.3 Energy distributions

The energy distribution of secondaries at a given depth depends on the radial distance from the shower axis. As a first approximation we integrate over the total area. We assume that the knowledge of the average energy is sufficient to determine the energy deposition in a given detector (for instance a scintillator). We remind in fact that for the aim of this work, the transverse dimensions of an e.m. sub-shower are in general much smaller than those of the whole EAS.

We have found that the energy distributions of secondary particles, at a given depth, are well approximated by the following expression:

$$\frac{dN_{e,\gamma}(E_0,t)}{dE} = C \cdot E^{\alpha(t)} \cdot e^{\beta(E_0,t)\cdot E^{\gamma}(t)} \tag{12}$$

where C is simply a normalisation constant, E_0 is the primary energy, and t is the atmospheric depth. Such an expression starts to underestimate the real distribution when this has decreased by at least two order of magnitude from the peak value.

The expressions α, β, and γ are functions of t and E_0, and depend upon the nature of both primary and secondary particles. Examples of the obtained results are given in Fig. 10 and 11 for 562 GeV sub-showers initiated by gamma and electrons respectively

We also notice how the knowledge of the energy distribution allows to scale the above mentioned longitudinal profiles down to any value of energy cut greater than 1 MeV.

In the following we give the parametrisation of all relevant functions for the four different cases. The variables $y = \log_{10} E_0$ and $x = 810 - 30.570 \cdot t$ are introduced.

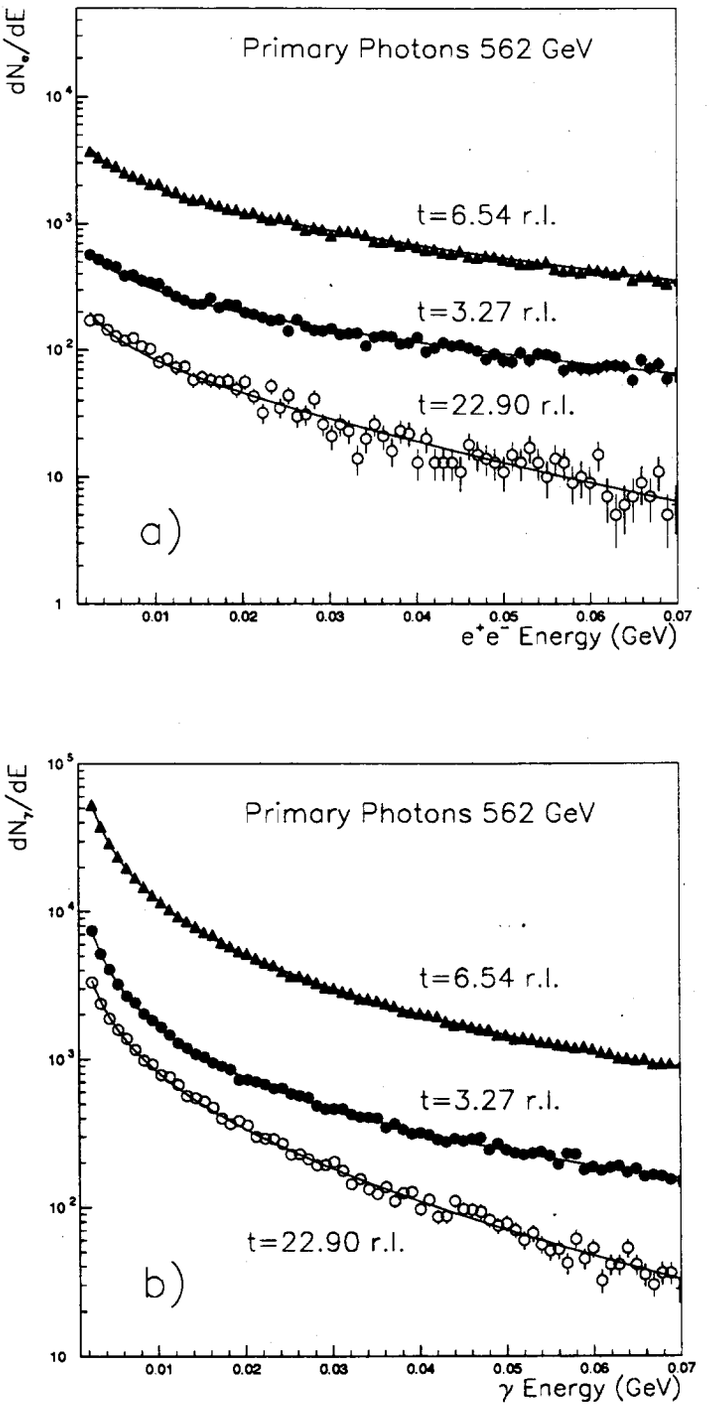

Figure 10: ***Energy distribution of secondary electrons (a), and photons (b), for photon-initiated sub-showers at 562 GeV at three different atmospheric depths.***

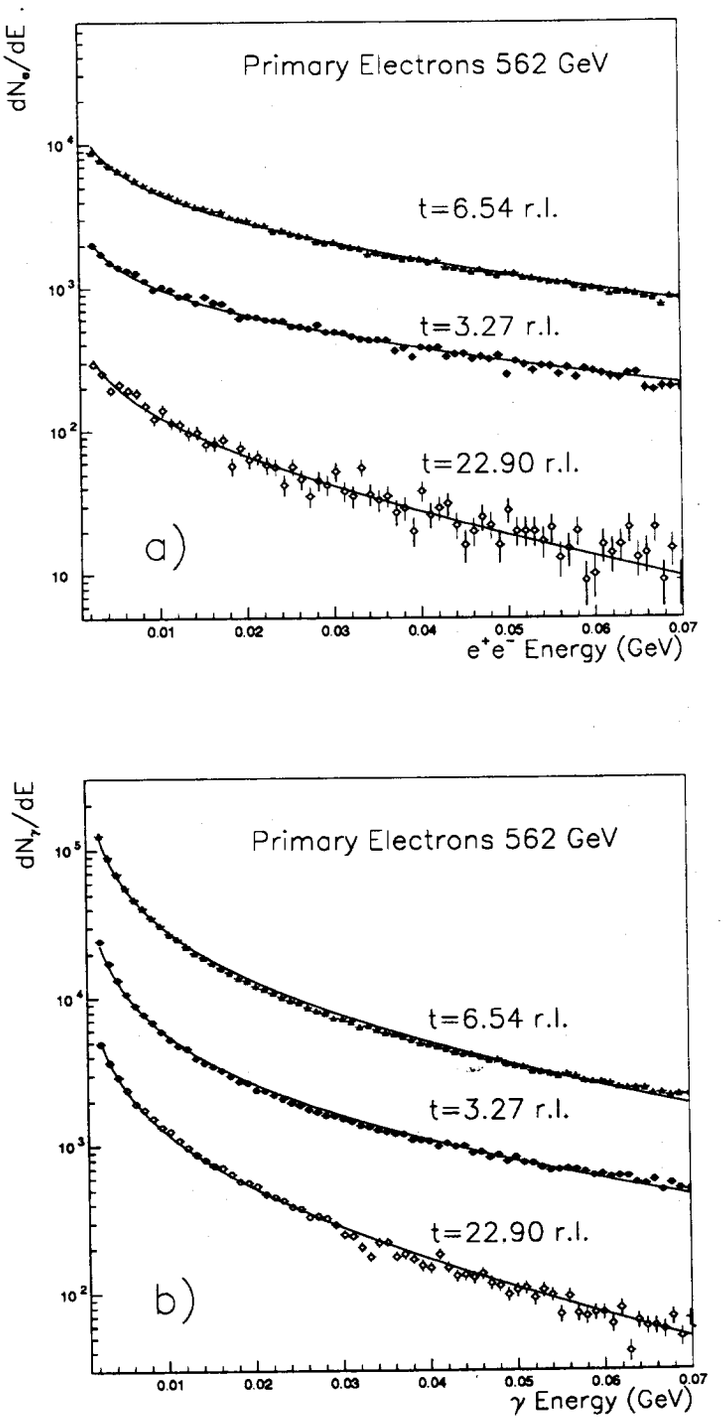

Figure 11: *Energy distribution of secondary electrons (a), and photons (b), for electron-initiated sub-showers at 562 GeV at three different atmospheric depths.*

3.3.1 Secondary e^+e^- from Primary Photons

$$\alpha(x) = -.4602 + .1458 \cdot 10^{-4} \cdot x \tag{13}$$

$$\beta(E_0, x) = p_0(E_0) + p_1(E_0) \cdot x \tag{14}$$

where p_0 and p_1 are given by:

$$p_0 = 34.692 - 2.47085 \cdot y - 1.6181 \cdot y^2 + .32336 \cdot y^3 \tag{15}$$

$$p_1 = -.32205 \cdot 10^{-1} - 1.8219 \cdot 10^{-3} \cdot y + 4.06915 \cdot 10^{-3} \cdot y^2 - 6.7065 \cdot 10^{-4} \cdot y^3 \tag{16}$$

In this case γ is a constant:

$$\gamma = 0.87 \tag{17}$$

3.3.2 Secondary γ from Primary Photons

$$\alpha(x) = -.81356 - .11373 \cdot 10^{-3} \cdot x \tag{18}$$

$$\beta(E_0, x) = c(E_0) \cdot (.229845 - 3.5588 \cdot 10^{-2} \cdot x + 1.6177 \cdot 10^{-5} \cdot x^2 - 6.608 \cdot 10^{-9} \cdot x^3) \tag{19}$$

where

$$c(E_0) = 1.1308 - .058528 \cdot y \tag{20}$$

$$\gamma(x) = .8856100 - .44941 \cdot 10^{-3} \cdot x + .30669 \cdot 10^{-6} \cdot x^2 - .13216 \cdot 10^{-9} \cdot x^3 \tag{21}$$

3.3.3 Secondary e^+e^- from Primary Electrons

$$\alpha(x) = -.488 + .56271 \cdot 10^{-4} \cdot x \tag{22}$$

$$\beta(E_0, x) = p_0(E_0) + p_1(E_0) \cdot x \tag{23}$$

where p_0 and p_1 are given by:

$$p_0 = 58.475 - 2.5329 \cdot y + 6.0455 \cdot y^2 - 5.3685 \cdot 10^{-1} \cdot y^3 \tag{24}$$

$$p_1 = -6.634 \cdot 10^{-2} + 3.2933 \cdot 10^{-2} \cdot y - 2.513 \cdot 10^{-2} \cdot y^2 + 6.741 \cdot 10^{-4} \cdot y^3 \tag{25}$$

Also in this case γ is a constant:

$$\gamma = 0.89 \tag{26}$$

3.3.4 Secondary γ from Primary Electrons

$$\alpha(x) = -.8846 - .7472 \cdot 10^{-4} \cdot x \tag{27}$$

$$\beta(E_0, x) = p_0 + p_1 \cdot x + p_2 \cdot x^2 + p_3 \cdot x^3 \tag{28}$$

where p_0, p_1, p_2, and p_3 are given by

$$p_0 = 50.235 - 13.144 \cdot y + 1.70655 \cdot y^2 + 3.49745 \cdot 10^{-4} \cdot y^3 \tag{29}$$

$$p_1 = -1.54705 \cdot 10^{-1} + 5.475 \cdot 10^{-2} \cdot y + 1.3477 \cdot 10^{-3} \cdot y^2 - 1.7199 \cdot 10^{-3} \cdot y^3 \quad (30)$$

$$p_2 = 3.12305 \cdot 10^{-4} - 7.5745 \cdot 10^{-5} \cdot y - 2.43885 \cdot 10^{-5} \cdot y^2 + 6.6675 \cdot 10^{-6} \cdot y^3 \quad (31)$$

$$p_3 = -2.3047 \cdot 10^{-7} + 3.1436 \cdot 10^{-8} \cdot y + 2.6297 \cdot 10^{-8} \cdot y^2 - 5.812 \cdot 10^{-9} \cdot y^3 \quad (32)$$

while γ is now:

$$\gamma = 1.0 \quad (33)$$

3.4 Lateral distribution

As expected the lateral distribution of secondary particles on a plane perpendicular to the shower axis is fitted, with reasonable approximation, by the Nishimura-Kamata-Greisen function[11]:

$$f(x) = N_e \cdot \frac{\Gamma(4.5-s)}{2\pi\Gamma(s)\Gamma(4.5-2s)} x^{s-2}(1+x)^{s-4.5} \quad (34)$$

where $x = r/r_0$. The paramters r_0 and s, as derived from the fit, are really close to the expected Moliere radius and age parameter respectively. An example of fit is shown in fig. 12, for secondary e^+e^- in a 1 TeV gammma initiated sub-shower, after an atmospheric depth of 460 gr/cm^2. This kind of function starts to overestimate the real distribution only at very large distances from the shower axis.

4 Conclusions

A successful parametrisation of some relevant features of e.m. showers in atmosphere has been presented. The aim of this work is to provide a set of tools to achieve fast and reliable simulation of the e.m. component of EAS for the analysis of Cosmic Ray Physics. In future papers we plan to extend such a work to a detailed analysis of lateral distribution and of arrival time fluctuations.

A dedicated effort will be reserved for the parametrisation of the e.m. component of hadronic sub-showers.

All correspondence can be sent to the following e-mail addresses:
patera@hpserver.lnf.infn.it
battist@hpserver.lnf.infn.it
carboni@hpserver.lnf.infn.it
ferraria@cernvm.cern.ch

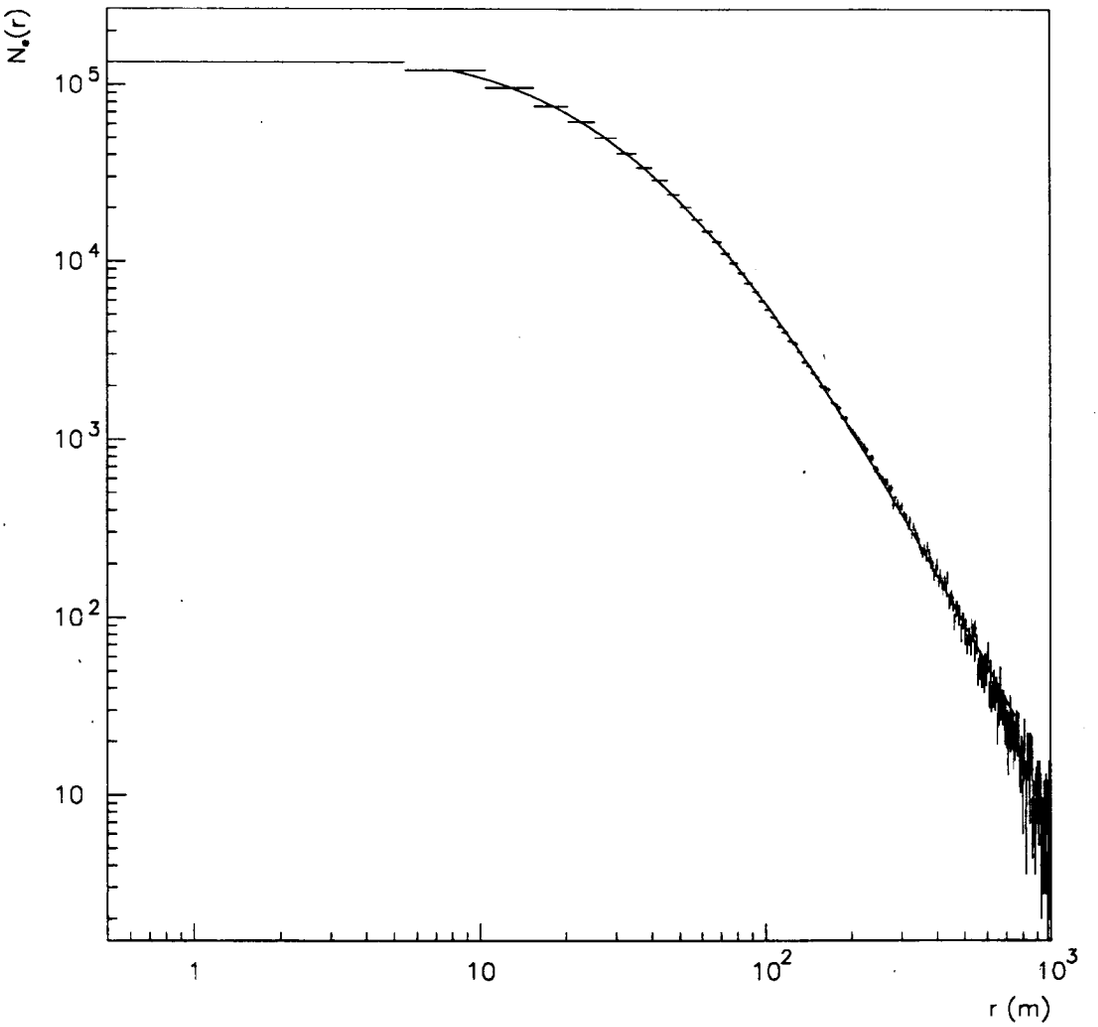

Figure 12: Radial distribution of secondary e^+e^- (E$\geq$ 1 MeV) for a 1 TeV gamma shower after 460 gr/cm^2. The fit to a NKG function is shown

5 Acknowledgments

Part of this work has been carried on by one of us (VP) at the California Institute of Technology. He wishes to express his gratitude to Prof. B. Barish and his coworkers for their kind hospitality. We are indebted to Prof. G. Navarra, Dr. S. Coutu and Dr. P. Vallania for many useful discussions.

References

[1] D. Müller et al., Proc. of the 22nd ICRC, Dublin (Ireland) 1991, OG 6.1.12, Vol. 2, 25, and reference therein.

[2] see for instance G. Battistoni, "Simulations in High Energy Cosmic Ray Physics",presented at the IV Int. Conf. on Calorimetry in High Energy Physics, La Biodola (Is. d'Elba), Italy, Sept. 20–25 1993, proceedings in press.

[3] T.K.Gaisser, "Cosmic Rays and Particle Physics", Cambridge University Press, Cambridge (UK) 1990, cap. 15 and references therein

[4] B. Rossi and K. Greisen, Revs. Mod. Phys. **13** (1941) 240.

[5] E. J. Fenyves et al., Phys. Rev **D37** no. 3 (1988) 649.

[6] C. Forti et al., Phys. Rev. **D42** (1990) 3668.

[7] H.P. Vankov and T. Stanev, Proc. 23rd I.C.R.C., Calgary, **4** (1993) 167.

[8] R. Brun et al., CERN GEANT 3 User's Guide, DD/EE/84-1 (1987).

[9] A. Fassó et al.,"Fluka: Present Status and Future Developments", presented at the IV Int. Conf. on Calorimetry in High Energy Physics, La Biodola (Is. d'Elba), Italy, Sept. 20–25 1993, proceedings in press.

[10] ref. [3], pag. 34

[11] K. Greisen, "Progress in Cosmic Ray Physics", vol. 3 (1956)

[12] W.T. Eadie, D. Drijard, F.E. James, M. Roos, and B. Saodulet,"Statistical Methods in Experimental Physics", North Holland, Amsterdam and London, 1971.